5th International Conference on Deep Foundation Practice, Singapore. pp 125-132

EMPIRICAL PILE DESIGN BASED ON CONE PENETROMETER DATA: AN EXPLANATION FOR THE REDUCTION OF UNIT BASE RESISTANCE BETWEEN CPTs AND PILES

X. Borghi[1], D.J. White[2], M.D. Bolton[2], S. Springman[1]
[1]Institute for Geotechnical Engineering,
Swiss Federal Institute of Technology, Zurich, Switzerland
[2]Geotechnical Engineering Research Group,
Cambridge University Engineering Department, UK

The cone penetration test (CPT) is regarded as an effective tool for pile design, since it resembles the penetration process of a pile. However, CPT resistance is significantly higher than the equivalent pile base resistance (quoted in units of stress). The paper describes an explanation for this scale effect, supported by a series of centrifuge tests that illustrate the phenomenon.

Keywords: CPT, pile design, base resistance, shaft friction, scale effect, base-shaft interaction, sand

1. Introduction

The axial capacity of a single pile has to be predicted for the design of a piled foundation. This requires the knowledge of appropriate soil parameters and their influence on both base and shaft resistance of a pile. The complexity of the penetration mechanism as well as the diversity of the governing parameters justifies the use of an empirical method based on in situ measurements. Design methods based on the Cone Penetration Test (CPT) allow the unit base resistance q_b of a pile to be correlated directly to the unit cone penetration resistance q_c. Since the CPT resembles the geometry and vertical penetration process of a pile, a one-to-one correlation of q_b and q_c seems intuitive. Several authors and recent design guidelines (e.g. [1], [2], [3], [4]) recommend that pile base resistance q_b should be taken to be equal to the cone resistance q_c.

This, however, has been shown to be inconsistent with field and laboratory observations. Indeed, the unit base resistance of a pile appears to decrease markedly as its diameter increases, so that a penetrometer (D=36 mm) has a much greater unit base resistance than the unit base capacity of a pile in the same soil. This trend is referred to as the base resistance scale effect. It has been demonstrated experimentally by Kerisel [5], Tejchman and Gwizdala [6], Meyerhof [7] and more recently by Chow [8] (Fig. 1). Her database of load tests reveals that the ratio of the pile to the penetrometer base resistance q_b/q_c may be as little as 0.4 for close-ended pile of diameter 600 mm. Hence, designing a pile with the oversimplified assumption that $q_b = q_c$ may lead to a dangerous overprediction of the pile capacity.

In order to account for this scale effect in design, a number of empirical correlations have been proposed, with the scale effect being attributed to a variety of parameters. A reduction factor, α, is used to reduce the value of q_c (Eq. 1). Often α is selected on the basis of soil type and density [9][10], independently of pile dimensions. Recently, Chow [8] published an empirical relation that links q_b and q_c accounting for the pile diameter D. De Nicola [11] proposes that α will be a function of in situ stress level (or depth). The basis for selecting reduction factors remains unclear, and there is no established explanation for the origin of the scale effect. None of the above quoted authors present a mechanism by which q_b/q_c tends to be less than unity. Faced with these three inconsistent approaches to account for the scale effect (soil type, pile diameter, pile depth) practising engineers have no basis for appreciating the conditions under which their determination of q_b from q_c may be conservative, unconservative or even hazardous.

$$q_b = \alpha\, q_c\ , (\alpha < 1) \qquad (1)$$

This paper aims to present an explanation for the base resistance scale effect, using simple theoretical considerations supported by the data of a centrifuge test series. A mechanism of stress interaction between the shaft and the base of the pile, which captures the base resistance scale effect, is presented. It is proposed that this mechanism offers a more rational framework for the prediction of pile base resistance from CPT data than has previously existed.

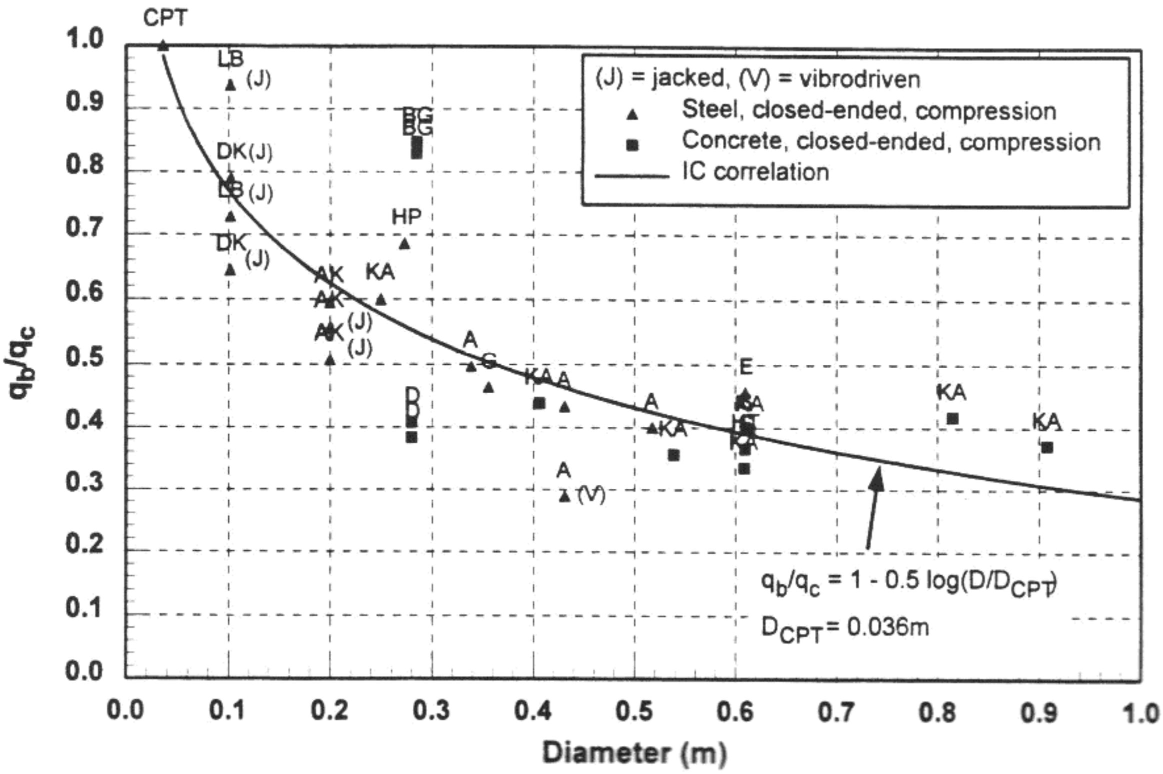

Figure 1: The base resistance scale effect (Chow, [8])

2. Hypothesis for scale effect

The scale effect may be explained through consideration of equilibrium in conjunction with elements of theoretical pile behaviour. According to bearing capacity solutions, the base resistance of a pile is proportional to the in situ vertical effective stress $\sigma'_{v,o}$ calculated as the self-weight of the soil overburden at the level of the pile base. Traditionally, equations of the form of (2) have been used to predict the pile base resistance.

$$q_b = N_q\, \sigma'_{v,o} \qquad (2)$$

Rudimentary design methods assume that the bearing capacity factor, N_q, is a function of soil friction angle ϕ' and is calculated on the basis of the limit equilibrium or slip-line failure of an assumed mechanism (e.g. [12, 13, 14]). However, it is widely accepted that these mechanisms do not represent the true mode of failure ([8], [15]). Bearing capacity mechanisms are often kinematically incomplete, ignore the influence of soil stiffness and compressibility, and the failure patterns do not match laboratory observations (e.g. [16], [17], [18]). However, more realistic methods for predicting base resistance based on a confined failure around the pile tip (e.g. [15], [19]) include a dependence on the ambient stress level, so a relationship of the form in equation 2 remains a sensible basis for analysis.

Shaft friction acting upwards on the pile shaft can equally be considered as a downwards drag on the soil adjacent to the shaft. This downward drag represents an additional component of vertical stress in the annulus of soil around the shaft. The cumulative effect of this downdrag when integrated over the pile length is to increase the confining stress around the advancing pile tip. From this higher confining stress, an increased base resistance would result according to equation (2). This effect can be incorporated into this analysis by rewriting the traditional bearing capacity solution as follows:

$$q_b = N_q \left(\sigma'_{v,o} + \sigma'_x \right) \quad (3)$$

The additional vertical effective stress at pile tip level due to downward shear stresses acting on soil adjacent to the pile is denoted σ'_x. A qualitative appreciation of the dependence of σ'_x on pile geometry can be obtained by considering the equilibrium of a cone-shaped zone of soil close to the pile base. This simplification allows the base-shaft interaction to be examined in an approximate manner. The width of the zone has been chosen to equal the approximate width of the zone of major deformation around an advancing pile observed during model tests [18]. Hence, dimension W in Figure 2 is taken as one pile diameter. Changes in ambient stress at greater horizontal distance from the pile will have a lesser effect on base resistance.

The height of the zone of interaction, L_x represents the vertical extent of the pile shaft from which shaft friction will contribute a significant component of additional vertical stress at the pile base. Shaft friction close to the pile base will be transmitted to the horizontal annulus of soil at the pile base level with little radial dissipation. Shaft friction from higher up the pile will be dissipated partly onto this annulus and partly beyond it. For the purposes of this qualitative analysis it seems pragmatic to simplify this complex load transfer function using a single variable, L_x. Since the extent of the annular zone of deformation is proportional to pile diameter, the height of the zone of interaction, L_x should also increase with pile diameter.

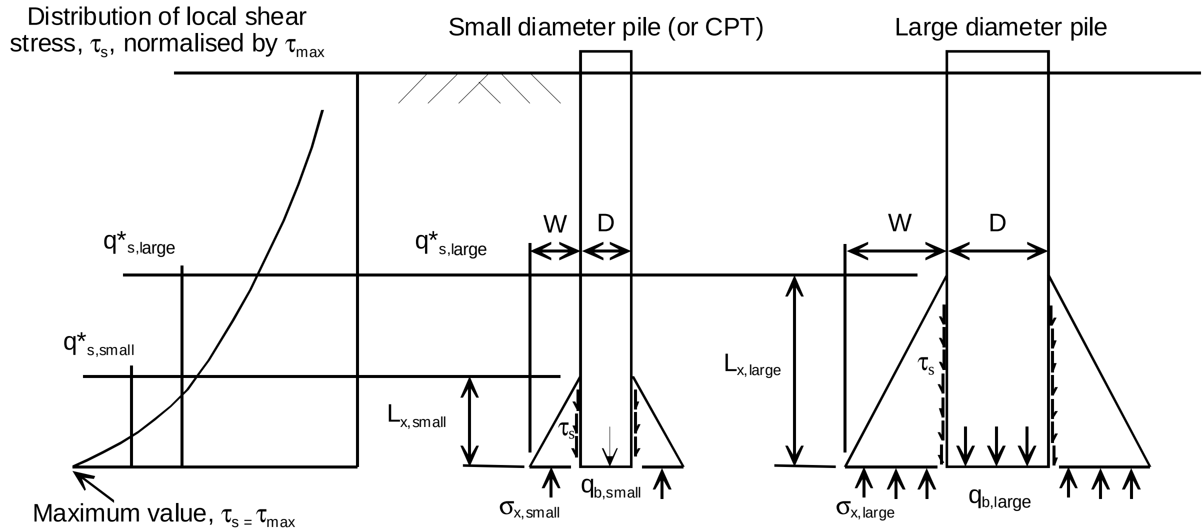

Figure 2: Schematic diagram of base-shaft interaction effect

Ignoring the shear stress acting on the inclined face of the cone, vertical equilibrium shows that σ'_x is proportional to the mean unit shaft resistance q^*_s developed along L_x. In this analysis, the local shaft friction profile is estimated by assuming that unit shaft friction at the pile base, τ_{max}, is proportional to the base resistance at that depth. As the pile penetrates further, the local shaft friction at a given depth decreases sharply from that initial value, following the qualitative profile shown in Figure 2. This follows the general trends observed by others (e.g. [8], [11], [15], [20]).

Having established an interaction zone (which links σ'_x and q^*_s) and an assumed distribution of shear stress along the pile shaft, the dependence of σ'_x on pile geometry can now be examined. Consider the two piles shown in Figure 2. Piles 1 and 2 are installed to identical depths, and have similar profiles of local shaft friction. It can be seen that the mean shaft friction, q^*_s, over the zone of interaction, is lower for the larger pile. This has the effect of creating a smaller increase in confining stress at the base, σ'_x. In turn, this leads to a lower value of q_b.

3. Centrifuge modelling

3.1 Overview of experiment

The experimental investigation used centrifuge modelling in order to replicate at laboratory scale the stress level found in the field. Four centrifuge tests were carried out during which different types of model pile were driven into a sand model. The aim of the test series was to observe the key feature of the above hypothesis i.e. the interaction between shaft friction and base resistance.

In order to observe this interaction, all the parameters that are traditionally thought to influence q_b were kept constant; identical soil at the same relative density was used in each test, and the cross-sectional area of the pile was kept constant. The only variable was the pile shaft roughness (i.e. the pile-soil interface friction angle). This permitted the installation of piles developing different unit shaft resistances. If no interaction between the shaft and the base existed, identical base resistance profiles would be recorded for all piles.

3.2 Experimental apparatus

The tests were performed on the geotechnical beam centrifuge at the Schofield Centrifuge Centre in Cambridge. The operation of the Cambridge 10 m diameter beam centrifuge, as well as the relevant scaling laws, are described in detail by Schofield [21]. To achieve the prototype dimensions described below, the tests were performed at a gravitational acceleration of 50g.

Four model piles were used; two of them had a smooth brass shaft (smooth piles SP) and two had a silica sand-coated shaft (rough piles RP), resulting in a much higher interface friction angle. All piles had a uniform shaft diameter of 12.5 mm including the sand coating for the rough piles. Each pile was 200 mm in length. In the 50g acceleration field, these dimensions correspond to a prototype pile diameter of 625 mm and an embedment depth of 10 m, which are typical characteristics of an on-shore pile. The pile tip was flat-ended (Fig. 3c). The rough sandy shaft was created by dropping silica sand (d_{50}=0.3 mm) onto the rotating, epoxy-coated brass tube.

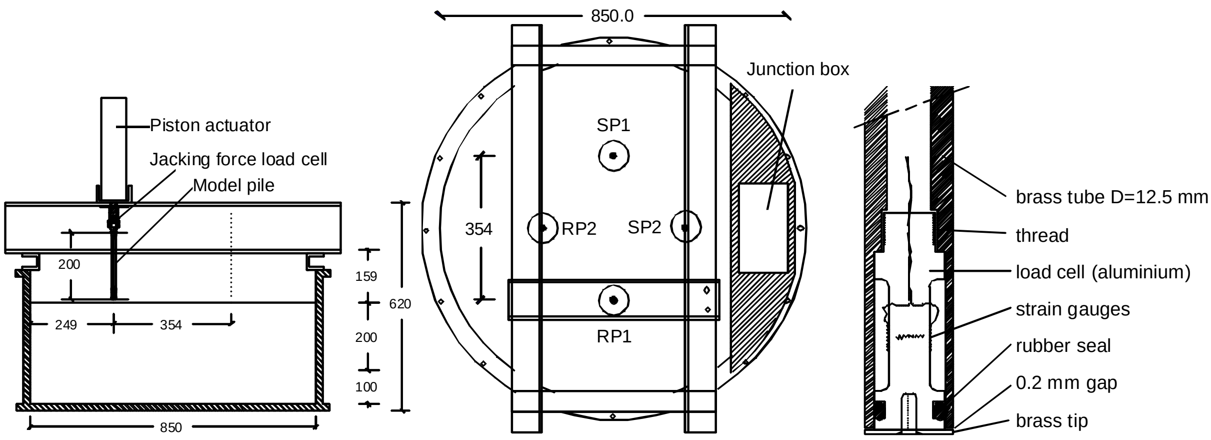

a) Cross-section of strongbox b) Plan view of strongbox c) Pile tip load cell

Figure 3: Experimental apparatus

The soil model was prepared by sand pluviation in a 850 mm diameter strong box (Fig. 3 a and b), which was placed on the centrifuge swing. A 300 mm deep bed of Dogs-Bay carbonate sand was rained at a controlled rate of 0.7 l/min from a constant drop height of 500 mm. The resulting sand model had a relative density of 89% (γ_d= 12.36 kN/m^3) and a voids ratio of 1.19 (e_{min}=1.14, e_{max}=1.71). Regular measurements taken during the sand pouring showed the relative density to be constant over the model depth. Dogs Bay sand is a biogenic carbonate sand, consisting predominantly of mollusc and foraminifera shells of a very angular nature, resulting in poorly graded particles and a high natural void ratio. This very compressible soil is described thoroughly by Coop and Lee [22] and Fookes [23].

The strong box was sufficiently large to allow all piles to be driven into the same soil model. Consequently, the results were not influenced by the possible variation in soil density if multiple soil models were used. The locations of each pile installation are shown on Figure 3b. A distance of 20 pile diameters was maintained between the installation point and the nearest side boundary and 8 diameters separated the pile tip from the bottom boundary when the full embedment depth was reached. Bolton *et al* [24] measured the influence of chamber size on axial load response and concluded that no significant boundary effect would occur if a distance of 11 pile diameters was maintained between model piles and the bottom boundary and if the ratio of chamber to pile diameter was greater than 40. The high compressibility of Dogs Bay sand indicates that an even smaller influence of the model boundaries than suggested by these Authors would be expected.

The jacking force was measured by a standard load cell of a capacity of 1.96 kN located between the pile and the actuator. Shaft friction was deduced by subtracting base resistance from the measured jacking force. Base resistance was measured directly by a load cell mounted in the pile tip (Fig. 3c). The tip load cell was designed to be interchangeable for all piles, to reduce the influence of multiple calibrations. The dimensions of the cell are shown in Figure 3c. Two pairs of 350 Ω strain-gauges formed a fully-active Wheatstone bridge circuit to provide compensation for temperature and bending-induced strains. All the transducers were carefully calibrated before and after the centrifuge tests and responded linearly throughout the relevant stress range, with no change in calibration factor during the test series. The model piles were jacked by means of a pneumatically operated piston actuator. The piston speed was controlled by draining the water contained in the bottom chamber of the piston through an adjustable pressure relief valve. A linear potentiometer, calibrated before and after the tests, recorded the extent of pile penetration. The data were recorded digitally at a sampling rate of 5 Hz using the Lab-tech notebook software package.

3.3 Experimental procedure

Following the swing-up of the model on the beam centrifuge, the centrifugal acceleration was increased to 50 g. The first pile (RP1) was then driven at 1 mm/s at the location indicated on Figure 3b. Once the full penetration was reached, the package was swung-down and the pile was carefully retrieved from the soil sample. The load cells were recovered, and set up on the next model pile (SP1). Subsequently, SP1 and 2 were installed, followed by RP2. The test programme was arranged so that any influence of installation sequence (stress cycling and interaction effects) would be evident in the differing response during the first (RP1) and final (RP2) tests.

4. Results of the centrifuge test series

4.1. Repeatability of data

The driving load Q_o, the total shaft friction Q_s and the unit base resistance, q_b, are plotted against pile tip depth, z_p, in Figures 4a, 4b and 4c. The jacking force required to install the rough piles was larger than anticipated. The maximum capacity of the actuator was exceeded after a penetration of 80mm. The smooth piles were installed to the full depth of 200mm.

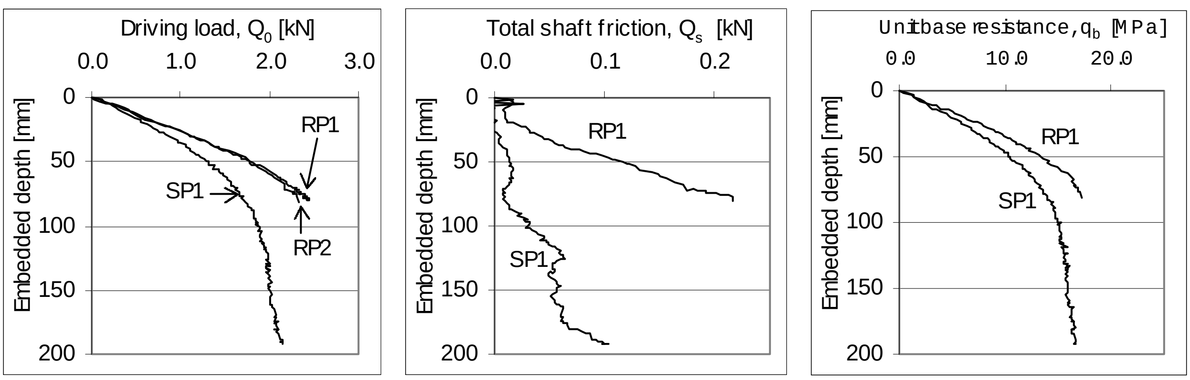

a) b) c)

Figure 4: Profiles of (a) driving load, Q_o, (b) shaft friction, Q_s, and (c) unit base resistance, q_b

The repeatability of the tests is indicated by the similar profiles of driving force for RP1 and RP2 (Figure 4a). For clarity, only the data from tests SP1 and RP1 are shown in subsequent figures. The measured normalised base resistance, q_b, ranges from 14 to 17 MPa for SP1 for depths of 80 to 200mm, or 4m to 10m full-scale, at which the pre-existing vertical effective stresses would have been 50 to 123 kPa. These figures conform with typical values for base resistance in calcareous sands close to their maximum relative density.

4.2. Influence of shaft roughness

Figure 4a indicates that the rough pile required approximately 30-40% more driving load than the smooth pile at corresponding penetrations. However, Figure 4b shows that this difference cannot be attributed simply to an increase in shaft friction. Although significantly greater shaft friction is developed on the rough pile, this contributes only 0.2 kN to the driving load of 2.3 kN at an embedment of 80mm. Figure 4c indicates that most of the additional resistance is developed at the base of the pile, with a 25% increase in base resistance being recorded.

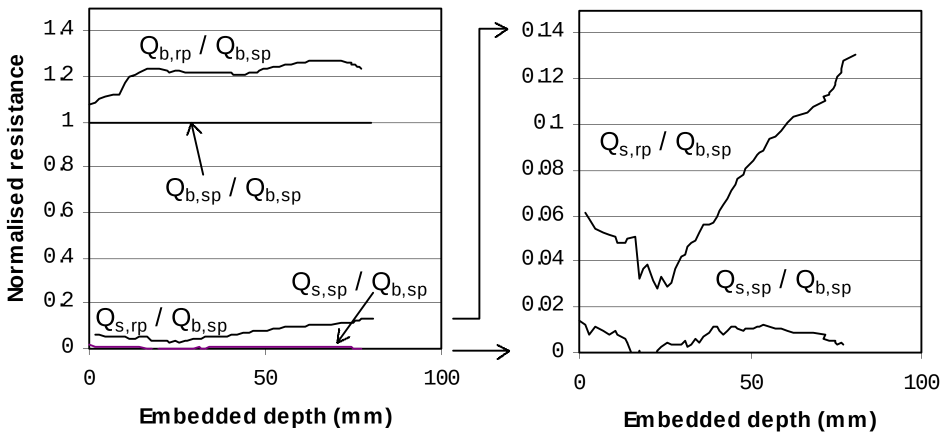

Figure 5: Normalised profiles of base resistance and shaft friction

The influence of shaft roughness is best demonstrated by normalising each profile by the base resistance on the smooth pile: see Figure 5. This could be considered as analogous to normalising each component by CPT resistance. Shaft friction is equal to around 1% and 10% of the base resistance of the smooth and rough piles respectively. Although roughening the shaft creates an order of magnitude increase in Q_s, the majority of the driving load is still due to base resistance. So, even though shaft friction represents only a small fraction of the driving load, it can create a significant increase in driving load through interaction with the base.

5. Analysis of results

In order to demonstrate the influence of the shaft friction on the tip resistance, simplified considerations of equilibrium are presented below. As explained in Section 2, the analysis should properly account for the actual unit shaft friction distribution in the vicinity of the pile tip, where it most contributes to the interaction with the base resistance. However, in the absence of local data for skin friction, and especially considering the need only to compare smooth and rough piles at a penetration of 80mm where the depth/diameter ratio is only 6, a simpler demonstration has been provided. The height L_x of the interaction zone in Figure 2 will simply be taken as the full penetration depth of the rough pile, 80mm. The total shaft friction Q_s will then be regarded as creating an extra vertical stress σ_x over an annulus defined arbitrarily by a semi-cone angle of 35° which thereby has a base area of 12200mm^2.

Table 1 sets out the required comparison between the rough and smooth pile, each driven 80mm. The usual analysis for N_q, ignoring the extra vertical stress σ_x, gives values 25% different for the rough and smooth piles at the same depth in the same soil. However, accounting for the shaft/base interaction through the enhancement σ_x the N_q values converge to within 7%.

		rough pile RP	smooth pile SP
q_b	MPa	**17.5**	**14.0**
$\sigma'_{v,o}$	kPa	**49.5**	**49.5**
Q_s	kN	**0.220**	**0.013**
σ_x	kPa	**18.0**	**1.0**
$\sigma'_{v,o} + \sigma_x$	kPa	**67.5**	**50.5**
$N_q = q_b / \sigma'_{v,o}$		**354**	**283**
$N_{q,corr} = q_b / (\sigma'_{v,o} + \sigma_x)$		**259**	**277**

Table 1: Demonstration of enhanced overburden stress effect σ_x on the calculation of N_q

6 Conclusions

Conventional methods of pile design based on CPT data often ignore the existence of the scale effect on base resistance, and assume that pile base resistance, q_b, is equal to CPT resistance q_c. Recent field data demonstrates that q_b/q_c decreases with pile diameter, indicating that design based on $q_b = q_c$ can be unconservative. However, no rigorous explanation for this phenomenon is available, and design correlations account which include the scale effect do so in an empirical manner.

It is hypothesised that interaction between shaft and base resistance close to the pile tip offers an explanation for the decrease in q_b/q_c with pile diameter. Considerations of equilibrium in the zone of soil around the pile base suggest that the downwards shear stresses on the soil close to the pile leads to an increased mean stress on the plane of the pile base. This effect varies with pile diameter. This increased mean stress leads to an increase in base resistance.

In order to demonstrate this base-shaft interaction effect, centrifuge model tests have been carried out. Two types of pile were jacked into a bed of dry sand. By varying only the pile-soil interface friction angle, the parameters which are conventionally accepted to govern base resistance were held constant. The results showed a distinct increase in unit base resistance with increased pile roughness. This indicates that base resistance is a function of shaft friction, confirming the hypothesis that interaction exists between the pile shaft and base. A tentative mechanism by which this effect can be quantified has been proposed. This mechanism offers a more rational framework for a design procedure which accounts for the scale effect than is currently available.

7 Acknowledgements

The authors would like to thank Chris Collison, Steve Chandler and the technical support team at the Schofield Centrifuge Centre for their expertise during the centrifuge test programme.

8 References

[1] BIDDLE, A.R. (1997) *The steel bearing piles guide*, 5th edition, Steel Construction Institute, Ascot, UK.
[2] TOMLINSON, M.J. (1998) *Foundation design and construction*, 6th edition. Pitman, London
[3] BOWLES, J.E. (1997) *Foundation analysis and design*, 5th edition, McGraw-Hill International Editions.
[4] FLEMING, W. G. K., WELTMAN, A. J., RANDOLPH M. F., & ELSON, W.K. (1992) *Piling Engineering* (2nd edition), Blackie Academic and Professional, Glasgow, UK.
[5] KERISEL, J. (1961) *Fondations profondes en milieux sablonneux: variation de la force portante limite en fonction de la densité, de la profondeur, du diamètre et de la vitesse d'enfoncement*, Proceedings 5th International Conference on Soil Mechanics & Foundation Engineering, Paris, Vol. 2, pp 73-83.

[6] TEJCHMAN, J.; GWIZDALA, K. (1979) *Analysis of safety factors of bearing capacity for large diameter piles*, Proceedings 7th European Conference on Soil Mechanics & Foundation Engineering, Brighton, U.K., Vol. 1, pp 293-296.
[7] MEYERHOF, G.G. (1983) *Scale effect of ultimate pile capacity*, Journal of the Geotechnical Engineering Division, ASCE 109(6), pp. 797-806.
[8] CHOW, F.C. (1996) *Investigations into the behaviour of displacement piles for offshore foundations*, PhD. Thesis, Imperial College, U.K.
[9] BUSTAMANTE, M.; GIANASELLI, L. (1982) *Pile bearing capacity by means of the static Penetrometer*, Proceedings 2nd European Symposium on Penetration Testing, pp 493-500.
[10] KRAFT L.M. *Computing axial pile capacity in sands for offshore conditions* Marine Geotechnology vol. 9 pp61-92
[11] DE NICOLA, A. (1996) *The performance of pipe piles in sand*, Ph.D. thesis, University of Western Australia, Nedlands 6907, Australia.
[12] TERZAGHI, K (1943) *Theoretical soil mechanics*. Wiley, J and Sons, New York.
[13] MEYERHOF, G.G. (1976) *Bearing capacity and settlement of pile foundations,* Journal of the Geotechnical Engineering Division ASCE 102(3), pp. 187-228.
[14] BEREZANTEV, V.C.; KRISTOFORNOF, V.; GOLUBKOV, V. (1961) *Load bearing capacity and deformation of piled foundations*, Proceedings. 4th International Conference on Soil Mechanics and Foundation Engineering, Paris, vol. 2, pp. 11-12.
[15] RANDOLPH M. F., DOLWIN J. & BECK R. (1994*) Design of driven piles in sand*, Geotechnique 44(3):427-448.
[16] ROBINSKY, E.I.; MORRISON, C.F. (1964) *Sand displacement and compaction around model friction pile,* Canadian Geotechnical Journal vol. 2, pp. 81-92.
[17] BCP Committee (1971) *Field tests on piles in sand, Soils and Foundations*, 11(2), pp. 29-49.
[18] KIRKHAM P.M. (1999) *Using CPT data to predict the behaviour of jacked piles*, Cambridge University MEng dissertation.
[19] SALGADO, R.; JAMIOLKOWSKI M.; MITCHELL, J.K. (1997) *Cavity expansion and penetration Resistance in Sand*. Journal of Geotechnical Engineering, ASCE 123(4), pp 344-354.
[20] TOOLAN, F.E., LINGS, M.L., MIRZA, U.A. (1990*) An appraisal of API RP2A recommendations for determining skin friction of piles in sand*, Proceedings 22nd Offshore Technology Conference, Houston, Texas OTC6422 4:33, pp. 33-42.
[21] SCHOFIELD, A.N. (1980) *Cambridge University geotechnical centrifuge operations*, Rankine Lecture, Geotechnique 30(3), pp. 227-268.
[22] COOP, M.R.; LEE, I.K. (1993) *Behaviour of granular soils at elevated stresses*, Wroth Memorial Symposium: Predictive Soil Mechanics, London, pp. 186-198.
[23] FOOKES, P.G. (1988) *The geology of carbonate soils and rocks and their engineering characterisation and description,* Proceeding of the International Conference on Calcareous Sediments, Perth, Australia, Vol. 2, pp. 787-806.
[24] BOLTON, MD, GUI, MW, GARNIER, J, CORTE, JF, BAGGE, G, LAUE, J, RENZI, R (1999) *Centrifuge cone penetration tests in sand,* Geotechnique 49 (4) pp 543-552